CHAPTER 4

STUDY OF THE EFFECT OF $PbO-B_2O_3-BaO-SiO_2$ GLASS ADDITIVE ON STRUCTURAL AND DIELECTRIC BEHAVIOUR OF $Ba_{0.5}Sr_{0.5}TiO_3$ CERAMICS

4.1 Introduction

In recent years, perovskite ceramics are in great demand for the manufacturing of next generation low cost ceramic products. Barium strontium titanate ($Ba_{0.5}Sr_{0.5}TiO_3$ (BST)) ceramic, which is a solid solution of $BaTiO_3$ and $SrTiO_3$, is one of the best example of perovskite ceramic which possess excellent properties such as high dielectric constant, low dielectric loss, high breakdown field strength, high tunability (non-linear dielectric under bias electric field), tunable transition temperature (by varying the Ba/Sr ratio) and better mechanical and thermal response. BST has Curie temperature below room temperature. It undergoes three different phase transitions similar to $BaTiO_3$ (cubic-tetragonal-orthorhombic-rhombohedral) but the transitions are shifted to lower temperatures. Only cubic structure is paraelectric and all other structure are ferroelectric [Jona and Shirane (1993)].

A ceramic material with low sintering temperature reduces the manufacturing cost at pilot scale. Controlled sintering conditions and effective sintering aid reduce sintering temperature and exaggerated grain growth. Liquid phase sintering (addition of low melting point glass to ceramic) is one of the best methods for decreasing sintering temperature without degrading its properties [Rani and Sebastian(2008); Armstrong et al. (1990); Zhang et al. (2004)]. The mechanism of liquid phase sintering is described in detail in section 1.8 of chapter 1. Multi-component glasses provide higher reduction in sintering temperature as well as better densification with good dielectric properties with

respect to single component glass [Anjana and Sebastian (2009)]. Khanna et al. (2014) and Wu and Huang (1999) have widely investigated the wide range of $PbO–B_2O_3–SiO_2$ glass. Borosilicate glasses form –Si–O–B–O– linkages to give continuous atomic structure and possess low dielectric loss and high impedance [Bijumon and Sebastian (2005)]. Both PbO and B_2O_3 in multi-component glasses reduces the viscosity of melt and increases the densification. Dielectric constant of glasses is stable within the microwave frequency range.

In the present investigation, novel $60PbO–20B_2O_3–5BaO–15SiO_2$ (PBBS) glass is synthesized and it has been utilized as the sintering aid for $Ba_{0.5}Sr_{0.5}TiO_3$ (BST) ceramic. The effects of PBBS glass addition on the sintering temperature, phase and dielectric properties of BST ceramic are investigated comprehensively.

4.2 Results and Discussion

The synthesis of different batch composition of $60PbO\text{-}20B_2O_3\text{-}5BaO\text{-}15SiO_2$ (PBBS) glass added $Ba_{0.5}Sr_{0.5}TiO_2$ (BST) ceramic was performed by solid state method. The detailed synthesis process has been mentioned in section 3.1 of Chapter 3. The nomenclature of different BST-PBBS batch compositions are given in Table 4.1. The detailed specification and description of the equipments used for the material characterisation such as density, phase, microstructure and dielectric properties are mentioned in section 3.2 of Chapter 3.

Table 4.1 Nomenclature of different BST-PBBS batch compositions

S.No.	Sample Composition	Nomenclature
1.	BST with 0 wt% glass	BST
2.	BST with 3 wt% glass	BST-3P
3.	BST with 5 wt% glass	BST-5P
4.	BST with 8 wt% glass	BST-8P
5.	BST with 10 wt% glass	BST-10P

4.2.1 Thermo-gravimetric and differential thermal analysis

Figure 4.1(a) shows the TG/DTA plot of ball milled powder of $Ba_{0.5}Sr_{0.5}TiO_3$ (BST) batch. TG shows continuous weight loss from 970K to 1250K. The DTA graph shows two weak endothermic peaks at 426K and 823K as well as two broad and strong endothermic peaks, which appears around 1060K and 1230K. The first endothermic peak observed at 426K corresponds to dehydration of moisture content present into the batch. The small peak at 823K corresponds to ~0.8% weight loss of the precursor and attributed to the decomposition of a very fine particle of $BaCO_3$ in the precursor. The endothermic peak around 1060K and the corresponding weight loss attributed to the decomposition of a very fine particle of $SrCO_3$. The raw material $BaCO_3$ and $SrCO_3$ have a fractional amount of finer particles that decompose at a low temperature in the presence of TiO_2. The endothermic peak present around 1230K corresponds to the complete decomposition of both $BaCO_3$ and $SrCO_3$ and reaction with TiO_2. Thus around 1230K perovskite BST starts forming [Balachandran et al. (2011); Rout and Panigrahi (2006); Vargas-Ortíz et al. (2012)].

Figure 4.1(b) shows the DTA traces of PBBS glass. The first endothermic peak is observed around 782K depicting the glass transition temperature (T_g). It was reported earlier that the glass transition temperature of $60PbO–20B_2O_3–20SiO_2$ glass is around 611K [Khanna et al. (2014)]. The BaO is acting as a network modifier and the addition of small concentration of network modifier to the B_2O_3 increases the glass transition temperature [Avramov et al. (2005)]. Two distinct and broad exothermic peaks around 1137K and 1230K are observed representing the crystallization temperatures (T_{C1} and T_{C2}) of glass. Second endothermic peak observed at 1308 K depict the glass melting temperature (T_m).

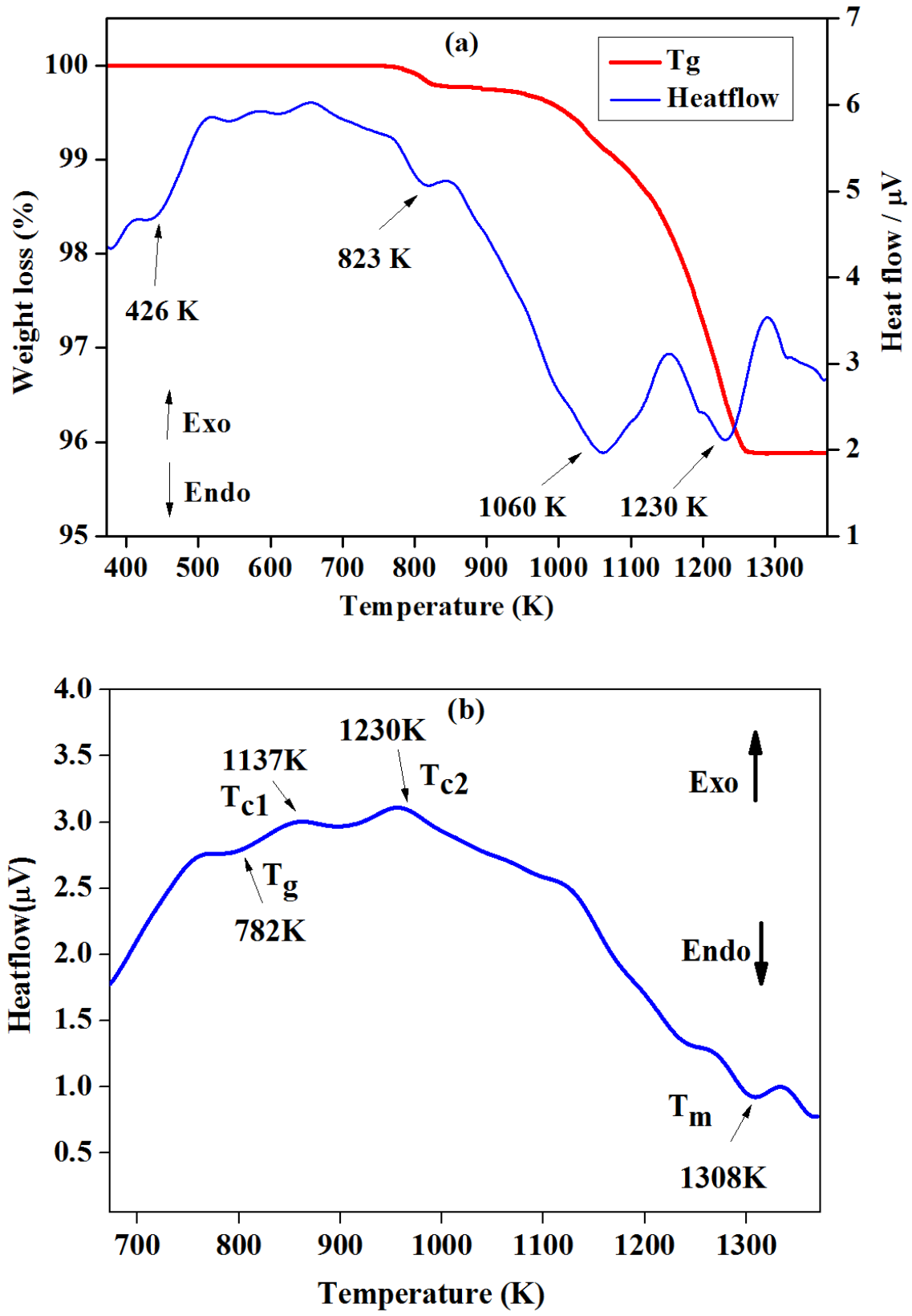

Figure 4.1 (a) DTA/TGA of $Ba_{0.5}Sr_{0.5}TiO_3$ and (b) DTA of PBBS glass.

4.2.2 Sintering and densification behaviour

Figure 4.2 shows the variation of percent relative density as a function of sintering temperature for all glass added BST (BST-3P, BST-5P, BST-8P and BST-10P) compositions. The inset of the figure 4.2 shows the variation of density with sintering temperature for the BST ceramic. Different BST ceramic specimens were sintered in the temperature range 1373 - 1573K and the maximum relative percentage density of 92.06% is obtained for the BST ceramic, which was sintered at 1523 K. The density of PBBS glass and BST were obtained as 5.789 g/cm^3 and 5.627 g/cm^3 respectively. The sintering experiments for (BST-3P, BST-5P, BST-8P and BST-10P) compositions were done in the temperature range 1100 - 1250K. It was found that the density of all the composition increases with increasing sintering temperature and increasing glass content. The density reaches a maximum up to a particular temperature and there after it decreases. The maximum relative percentage densities for different composition is given in Table 4.2. The relative density for BST-10P composition sintered at 1148K is maximum. It is observed from the graph that the addition of glass phase accelerated the densification of BST ceramic at significant lower sintering temperatures. Low sintering temperature of the ceramic is preferred as it reduces the production cost at medium to large scale. Addition of glass increases the density because liquid form of glass penetrates the solid particles of ceramics to spread uniformly, fill the pores and form bridges between the grains. It is also observed that the density increases with increasing sintering temperature upto maximum value then start decreasing. Decrease in density after reaching certain maximum value may be due to the excessive grain growth and crystallization of glass reducing densification and increasing porosity [Anjana and Sebastian (2009)].

Table 4.2 The maximum relative percentage densities for different compositions

Sample Code	Sintering Temperature	Relative Density (%)
BST	1523 K	92.06
BST-3P	1223 K	83.9
BST-5P	1198 K	85.5
BST-8P	1173 K	88.8
BST-10P	1148 K	90.2

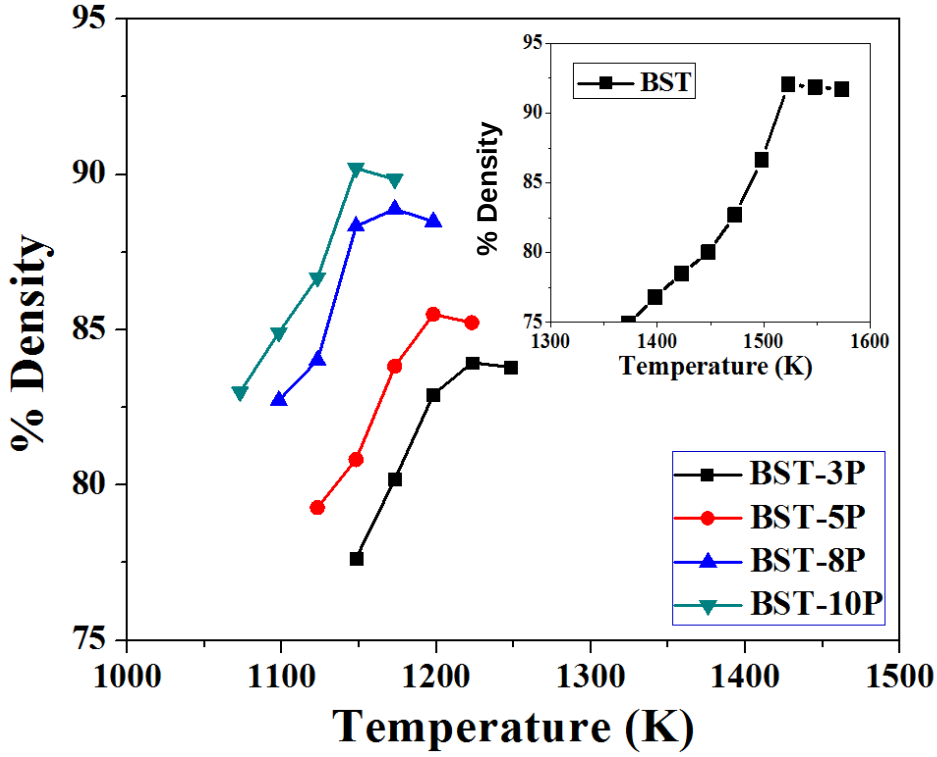

Figure 4.2 Variation of density with sintering temperature of samples BST, BST-3P, BST-5P, BST-8P and BST-10P.

4.2.3 Phase analysis

The calcination of $Ba_{0.5}Sr_{0.5}TiO_3$ (BST) ceramic was performed at 1273K. The XRD patterns of calcined powder (Figure 4.3(a)) confirms the formation of BST phase. Figure 4.3(b) shows the XRD pattern of BST sample sintered at 1523K. All XRD peaks are matched with JCPDS file no: 39-1395, which confirms the formation of single phase perovskite BST ceramic. Rietveld analysis for XRD data of BST was carried out for structure refinement. Rietveld analysis plays a great role for the identification of crystal structure including other structural information. Basic idea behind the refinement is to compare the actual powder diffraction pattern with simulation diffraction pattern. Refinement result confirm the single cubic phase formation of BST with space group Pm3m and lattice parameter a = b = c = 3.9525Å ± 0.05%. The unit cell volume, density and crystallite size of BST are 61.746$Å^3$, 5.18 g/cm^3 and 51 nm respectively. Wyckoff position and crystallographic details are mentioned in the Table 4.3. The goodness of fit (χ^2) value is 1.51 indicating satisfactory refinement results. Figure 4.3(c) shows the comparative XRD pattern of liquid phase sintered BST samples. No secondary peak is observed in the XRD patterns. It is clear from the figure 4.3(c) that addition of different wt% (3, 5, 8, and 10) of glass has no effect on the diffraction patterns and the crystal structures of BST phase.

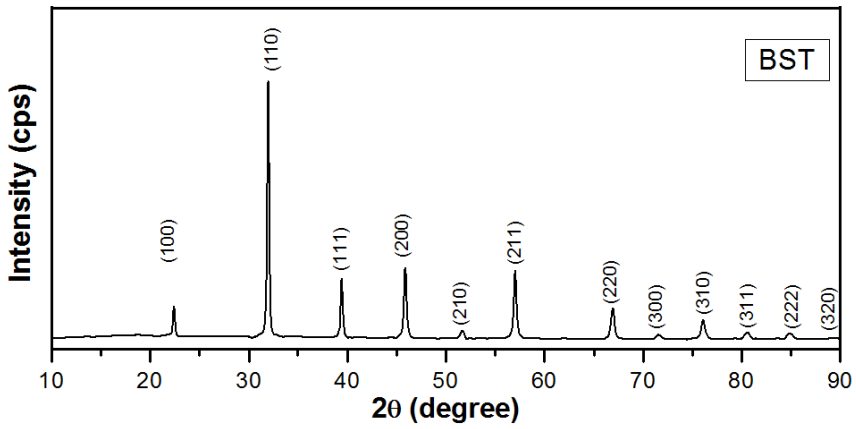

Figure 4.3(a) XRD pattern of calcined $Ba_{0.5}Sr_{0.5}TiO_3$ powder sample.

Table 4.3 Wyckoff position and crystallographic details of BST.

Name of Sample	Space Group	Crystal System	Atoms	Site	X	Y	Z
BST	Pm3m	Cubic	Ba	1a	0.0	0.0	0.0
			Sr	1a	0.0	0.0	0.0
			Ti	6c	0.5	0.499	0.5
			O	3c	0.0	0.5	0.5
Goodness of fit (χ^2) and lattice parameter details of BST							
Cell Parameter (a=b=c) (Å)	**Bragg R-factor**	**RF-factor**	**R_p**	**R_{wp}**	**R_e**	**χ^2**	**Cell Angle (α=β=ϒ)**
3.952489	20.8	12.75	30.9	29.4	23.91	1.51	90°

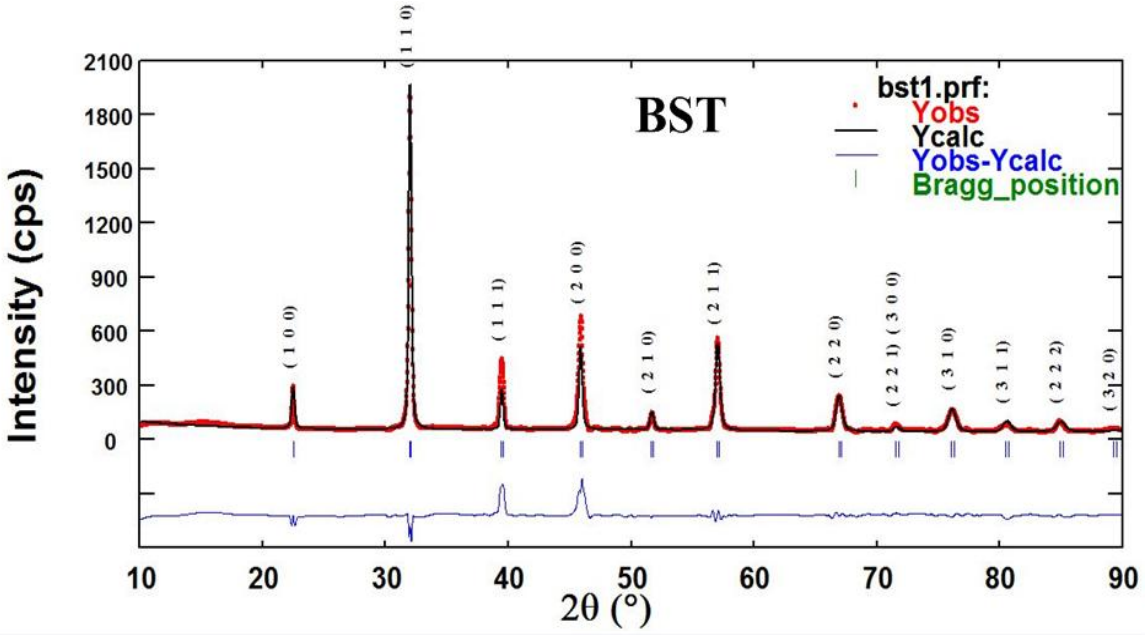

Figure 4.3(b) XRD pattern of $Ba_{0.5}Sr_{0.5}TiO_3$ sintered at 1523K.

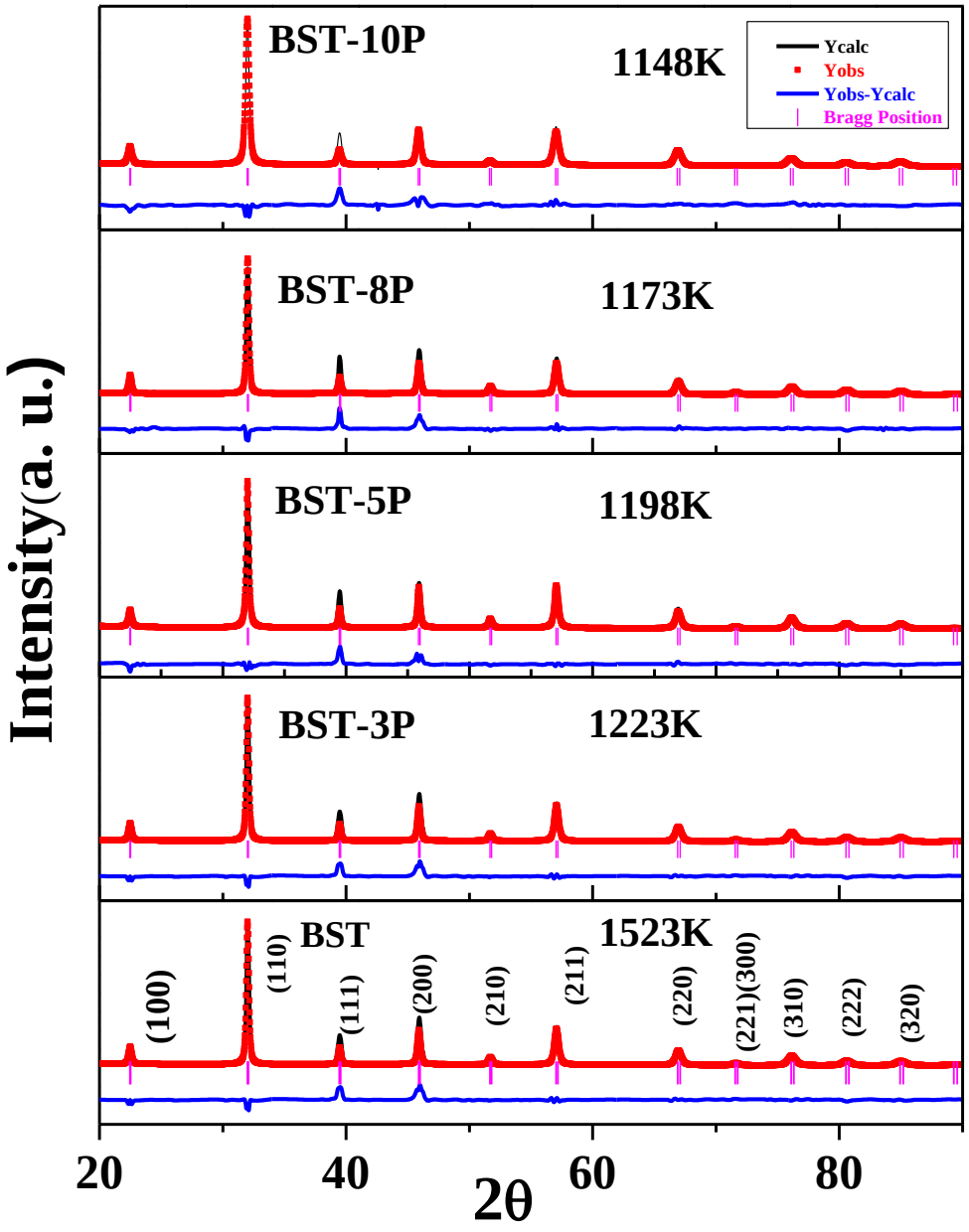

Figure 4.3(c) Comparative XRD analysis of different sample BST, BST-3P, BST-5P, BST-8P and BST-10P sintered at 1523K, 1223K, 1198K, 1173K and 1148K, respectively.

4.2.4 Microstructure

Figure 4.4 shows the SEM microstructure of all sintered samples at 10K magnification. The microstructure clearly shows the grain growth in all samples with average grain size in micrometre range. The microstructure clearly shows the exaggerated grain growth (~8 μm) and heterogeneous grain distribution in BST ceramic sample (figure 4.4(a)). In BST-3P, very small grains of around ~1 μm is observed while in BST-5P, again the grain size increases (~2 μm) along with its homogeneous distribution throughout the ceramic matrix. Homogeneous grain distribution is observed for all glass added ceramic compositions as compared to BST ceramic.

Figure 4.4 indicates the effectiveness of glass as a sintering aid. Figure 4.4 (b-e) shows that PBBS glass addition not affected (no secondary phase) the crystal structure of BST. The grain uniformity decreases with the increase in the weight percent in glass; which can be attributed to the liquid phase effect of glass observed at the grain boundaries. Sample (BTS-10P) shows maximum density, which is also verified from measured and theoretical density. It may be concluded that the glass concentration plays an important role on densification and enhancement of grain size of BST. Therefore glass is regard to act as effective sintering aid for the BST ceramics.

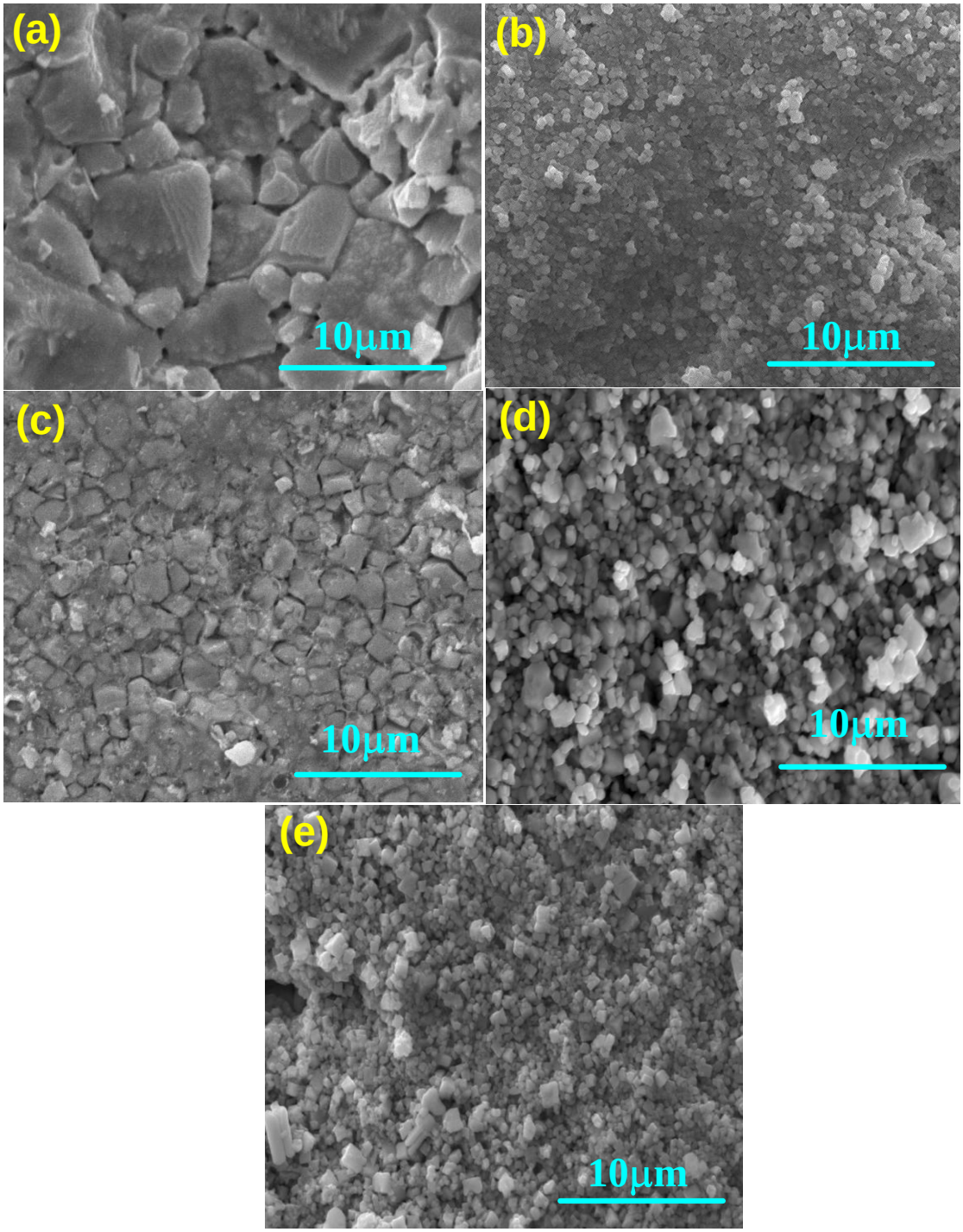

Figure 4.4 SEM microstructure of (a) BST, (b) BST-3P, (c) BST-5P, (d) BST-8P and (e) BST-10P.

4.2.5 **Analysis of dielectric property**

Figure 4.5 and 4.6 shows the measured variation of dielectric constant and loss tangent (inset) as a function of temperature at different frequencies (1 KHz, 10 KHz, 50 KHz, 100KHz and 1 MHz) for all the sintered samples (BST – BST-10P) within the temperature range of 20 - 293K and 293-450K, respectively. It is observed from Figure 4.5(a-e) that dielectric constant value increases with increasing temperature up to the transition temperature. This trend is so because of thermally activated relaxation behaviour [Nhalil et al. (2015)]. Above transition temperature, dielectric values decreases with increasing temperature due to disappearance of domains as shown in Figure 4.6 (a-e). The transition temperatures of all compositions are found below the room temperature which depicts their paraelectric phase at and above room temperature. There are many factors that influence the frequency dependent dielectric constant i.e. compositional fluctuation, interfacial polarization and micro domain softening [Adhlakha et al. (2014)]. At higher frequency, charge carrier dominates the probability of interwell hopping. There might be existence of heterogeneous distribution of charge carrier which decreases the value of dielectric constant at higher frequencies [Adhlakha et al. (2014)]. Figure 4.5 shows that BST, BST-5P and BST-8P possessed relaxation behavior. It is depicted from inset of Tanδ Vs frequency graph of figure 4.5(a, c and d) that at higher frequency, relaxation time decreases with temperature which indicates faster polarization with increase in dipole density.

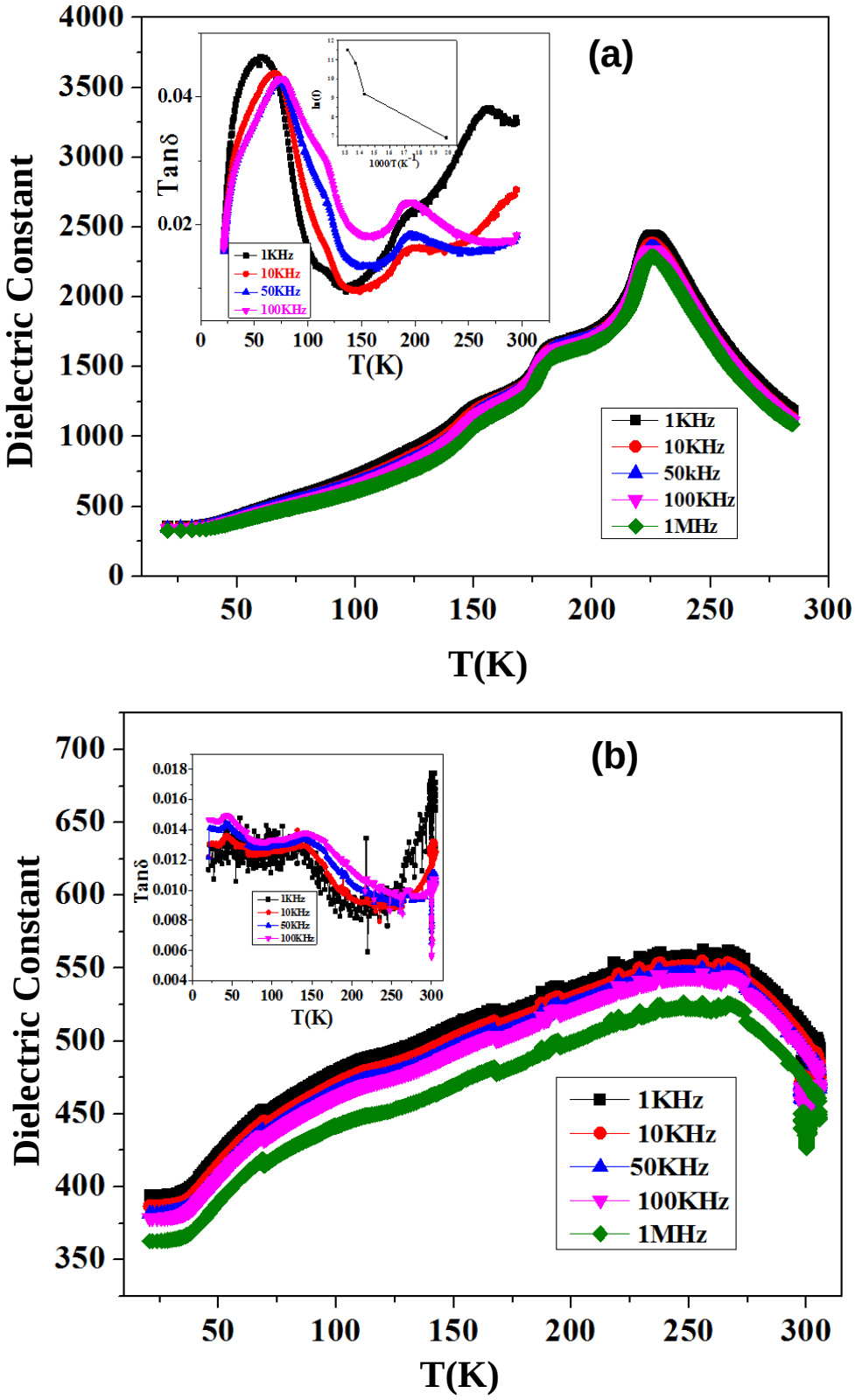

Figure 4.5 Variation of dielectric constant and loss tangent with temperature within the temperature range of 20K to 293K at different frequencies for the ceramic samples: (a) BST and (b) BST-3P.

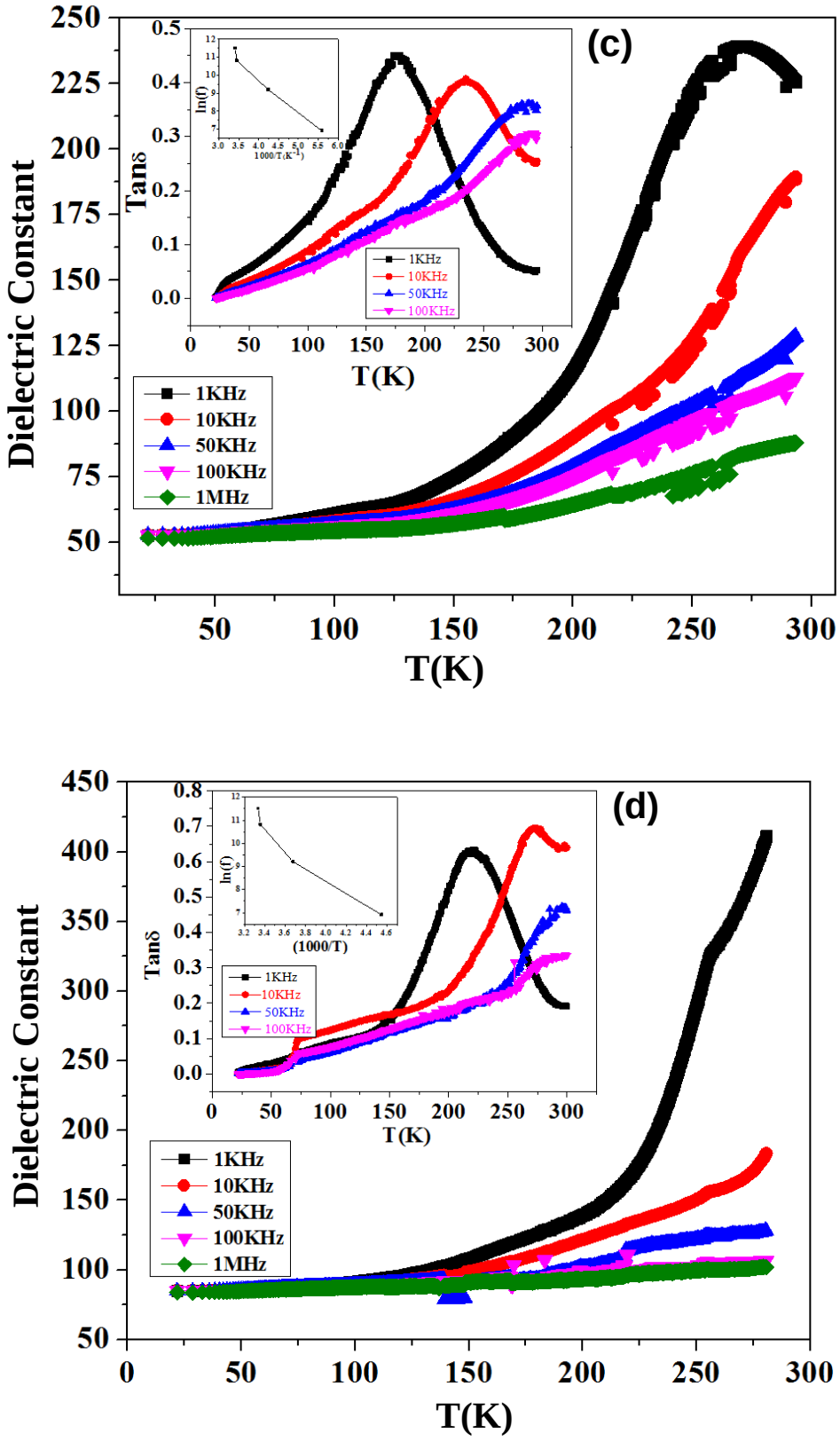

Figure 4.5 (contd): Variation of dielectric constant and loss tangent with temperature within the temperature range of 20K to 293K at different frequencies for the ceramic samples: (c) BST-5P and (d) BST-8P

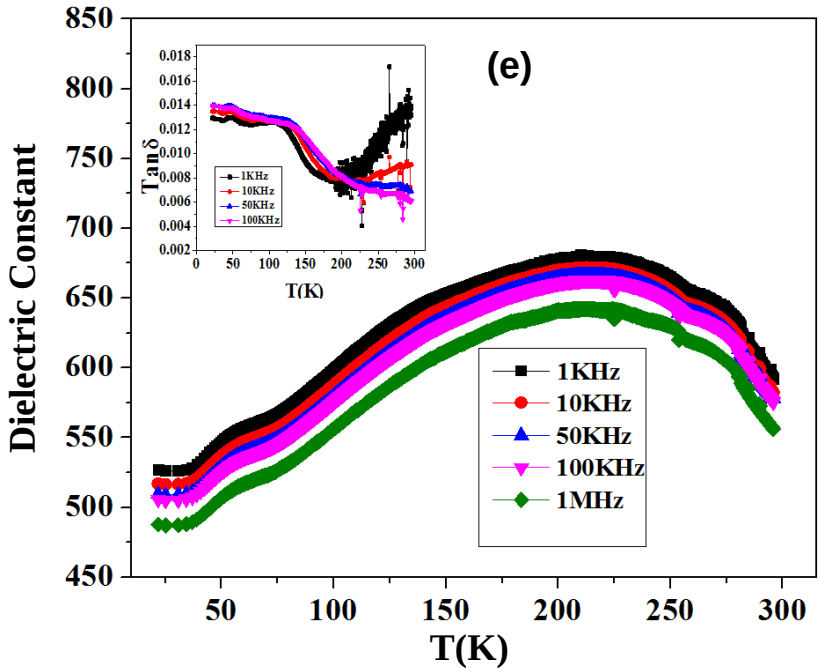

Figure 4.5 (contd.): Variation of dielectric constant and loss tangent with temperature within the temperature range of 20K to 293K at different frequencies for the ceramic sample (e) BST-10P.

$BaTiO_3$ shows three polymorphic transitions at 393K, 288K and 197K, respectively [Jona and Shirane (1993)]. Due to doping of 0.5 mole fraction strontium at Ba site, the transition temperature shift to 225K, 182K and 152K, respectively as shown in figure 4.5(a). The transition temperature shifted due to phase transformation within the BST sample. The ferroelectric to paraelectric phase transition for BST-3P, BST-5P, BST-8P and BST-10P are found at 267K, 271K, 257K and 229K, respectively. Figure 4.7(a and b) shows the comparison of dielectric values of BST, BST-3P, BST-5P, BST-8P and BST-10P samples as a function of temperature at 1 MHz. It is observed that dielectric constant initially decreases with increasing glass concentration up to 5 wt% and then start increasing with further increase in glass concentration (>5 wt%). When small amount of glass (3 wt%) added into the BST, the dielectric constant decrease suddenly by large value. This is because of introduction of other phase (glass with low dielectric constant) decreases the effective dielectric constant by mixture rule. The trend is followed up to BST-5P (5 wt% addition of glass).

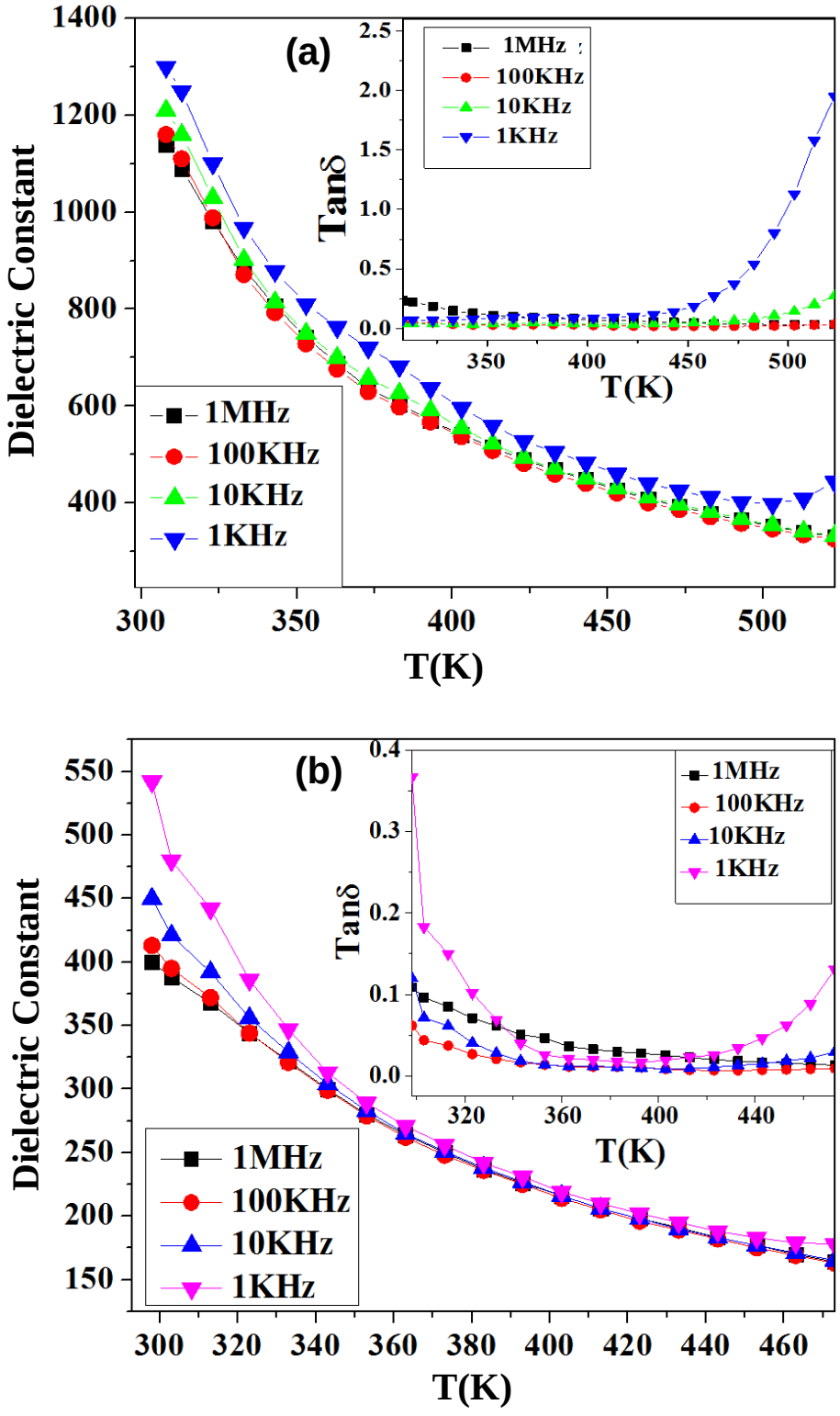

Figure 4.6 Variation of dielectric constant and loss tangent with temperature within the temperature range of 293K to 450K at different frequencies for the ceramic samples: (a) BST and (b) BST-3P.

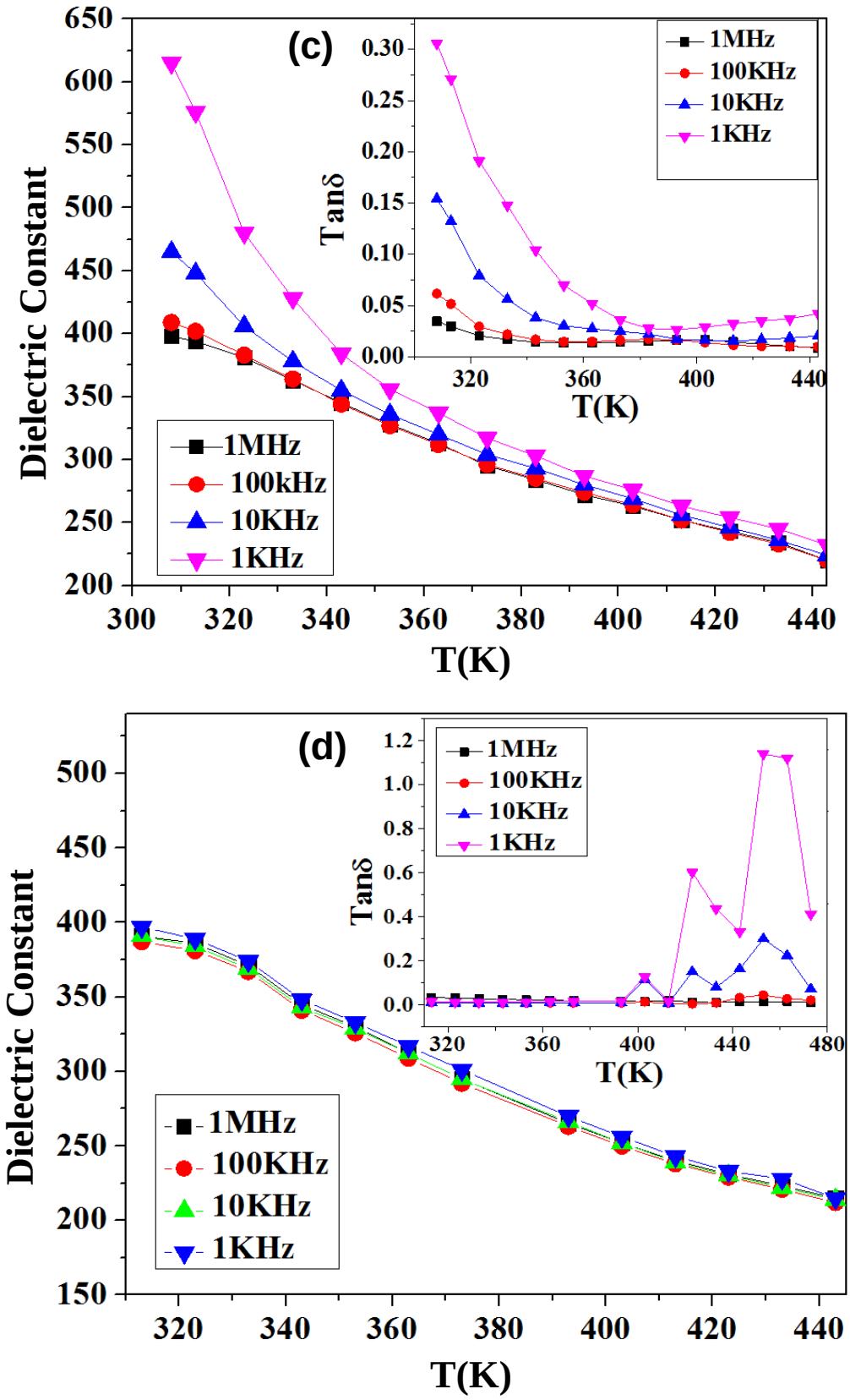

Figure 4.6 (contd.) Variation of dielectric constant and loss tangent with temperature within the temperature range of 293K to 450K at different frequencies for the ceramic samples: (c) BST-5P and (d) BST-8P.

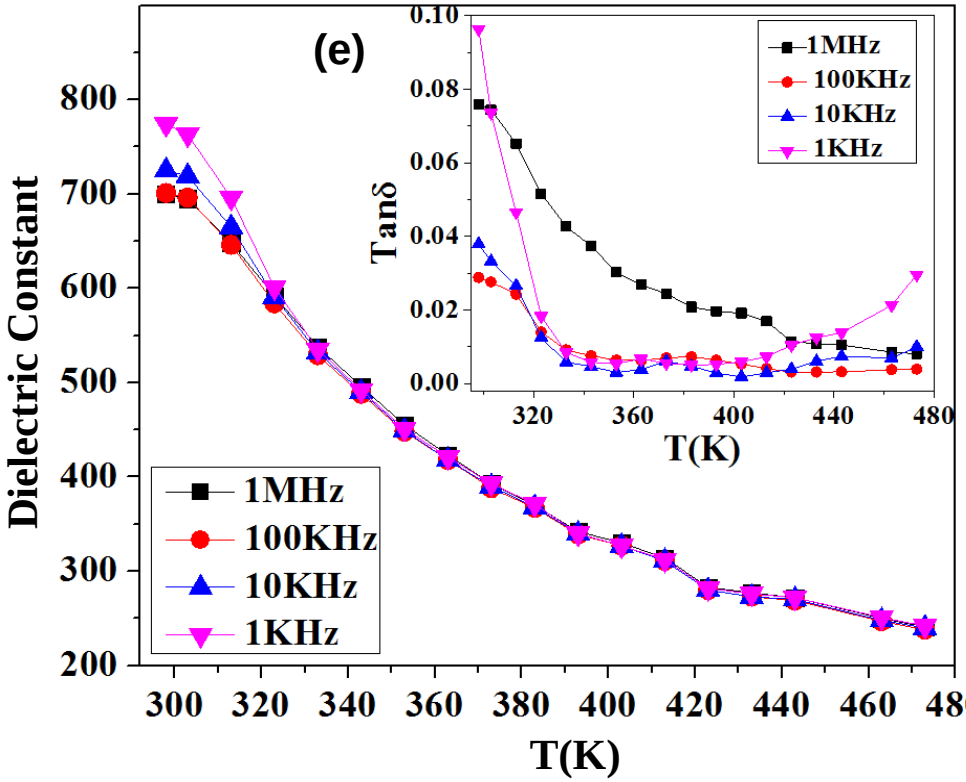

Figure 4.6 (contd.) Variation of dielectric constant and loss tangent with temperature within the temperature range of 293K to 450K at different frequencies for the ceramic sample: (e) BST-10P.

Further increase of glass concentration increases density causes increases dielectric constant. It is also observed that glass addition affects the transition temperature. By increasing the glass concentration up to 5 wt%, transition temperature shifted towards higher temperature. Further increase of glass concentration (>5 wt%), transition temperature shifted towards lower temperature side. Shifting of transition temperature towards higher temperature side may be due to Pb and/or Ba content of glass trying to enter into the lattice of BST. Increasing concentration of glass above 5 wt% increases the density significantly without affecting the lattice of BST which causes shifting the transition temperature towards lower temperature side. Insets of figures 4.5(a-e) and 4.6(a-e) shows variation of dielectric loss with temperature. It is also observed from figures 4.5 & 4.6 that transition temperature of all composition is below the room temperature. Thus all composition shows paraelectric behaviour at room temperature.

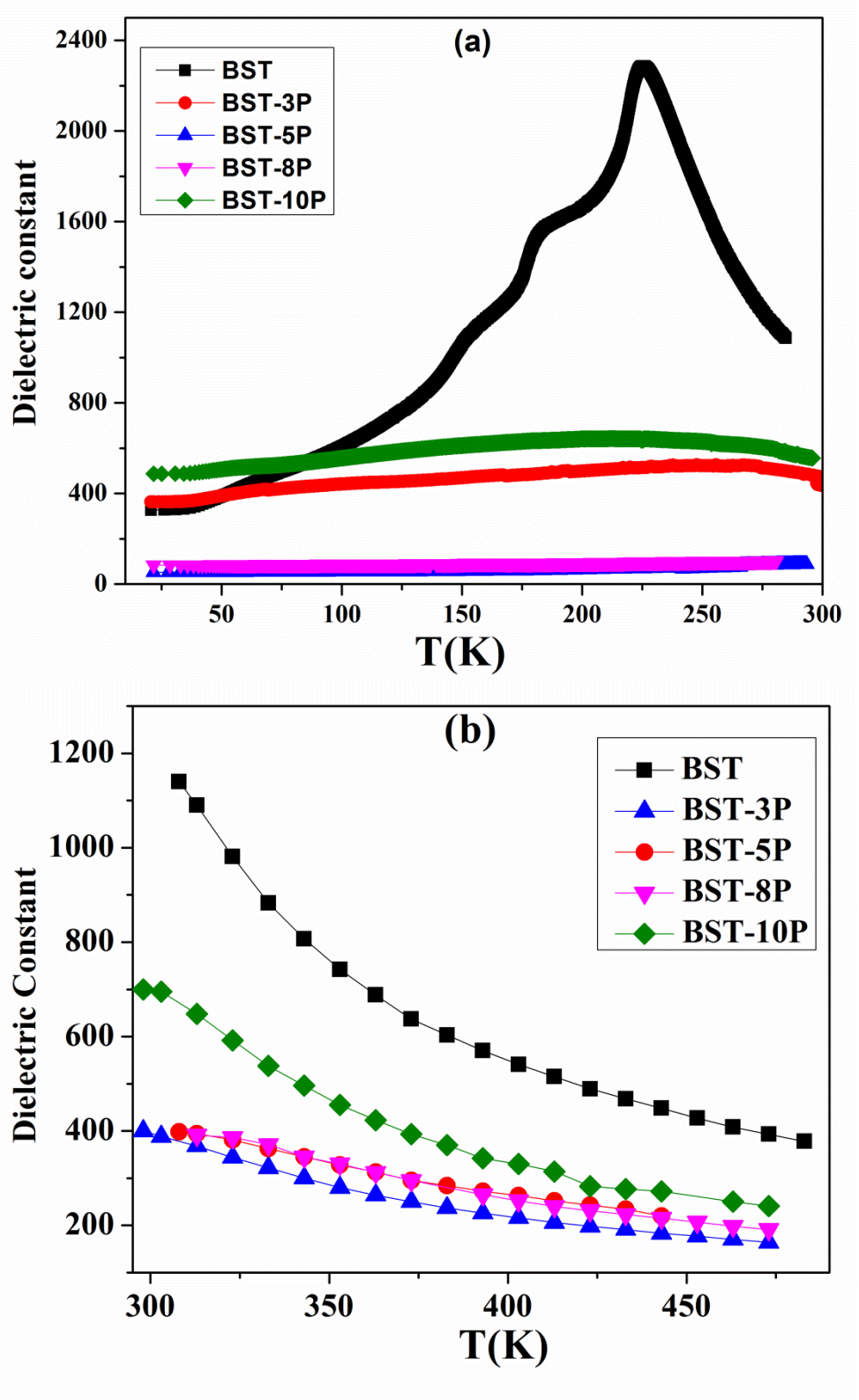

Figure 4.7 Variation of dielectric constant with temperature of different ceramic samples at 1 MHz at (a) 20 to 293K and (b) 293K to 450K.

Figure 4.8(a) shows the dielectric variation as a function of frequency within the microwave frequency range 8.5 - 11 GHz at room temperature. It is observed that dielectric values are almost constant over the entire frequency range. However, a little variation is observed, which may be due to heterogeneous grain distribution along with non-uniform stress concentration [Tripathi et al. (2018), Wee et al. (2011)]. The dielectric values of all samples are very low at GHz frequencies, when compared with MHz or lower frequencies because of only atomic and electronic polarization contribute to dielectric constant at GHz frequencies. It is also observed from the graph that dielectric constant decreases with increase in glass concentration up to BST-5P (5 wt%) and then starts increasing with further increase of glass concentration up to 10 wt% (BST-10P). The variation of loss tangent as the function of frequencies is shown in figure 4.8(b). The average dielectric constant and dielectric loss for the BST ceramic compositions and PBBS glass, are given in Table 4.4. BST-10P shows stable and highest dielectric constant of 27 with lowest dielectric loss ($\tan\delta \sim 0.121$) as compared with other glass added BST compositions.

Table 4.4 Dielectric properties of BST ceramic compositions and PBBS glass (8.5 – 11GHz)

S.No.	Material	Average Dielectric constant	Average Dielectric loss
1.	PBBS glass	5.8	0.090
2.	BST	84	0.013
3.	BST-3P	15	0.354
4.	BST-5P	13.8	0.596
5.	BST-8P	25.8	0.237
6.	BST-10P	27.0	0.121

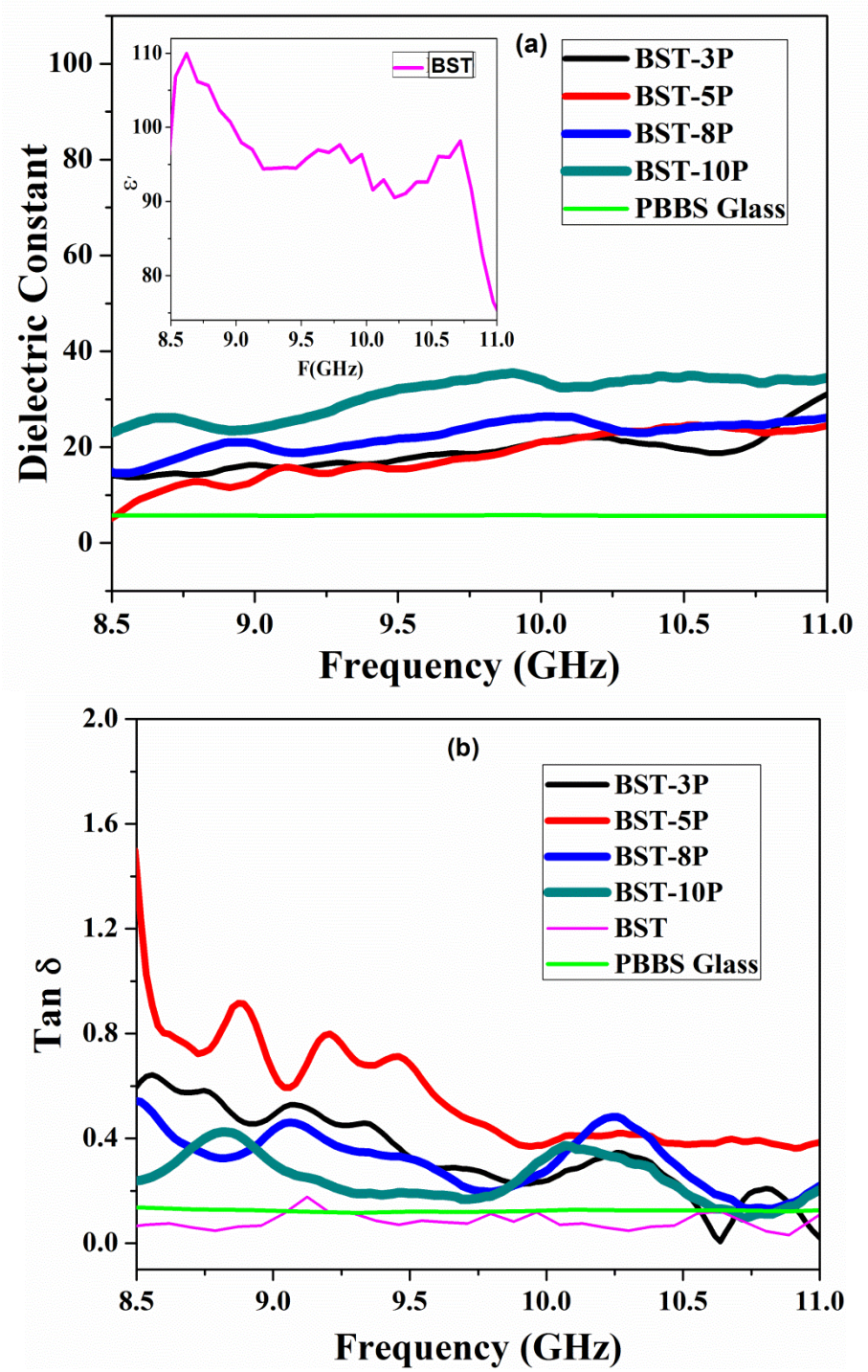

Figure 4.8 Variation of (a) dielectric constant and (b) Loss tangent of different ceramic samples with frequencies in GHz range.

4.3 Summary

In this chapter, increasing amount (3, 5, 8 and 10 wt%) of PBBS glass added $Ba_{0.5}Sr_{0.5}TiO_3$ (BST) ceramic are synthesized and investigated. Increasing weight percentage significantly reduces the sintering temperature of BST. Composition BST-10P shows the highest density with lowest sintering temperature as compared with all other composition. XRD analysis revealed that addition of PBBS glass has no effect on the crystal structure of BST. Analysis of dielectric property has reveals that transition temperature was increased with increase in glass concentration up to 5 wt% and then starts decreasing by further increase of the glass concentration (>5 wt%). Transition temperature also shifted towards higher temperature side on increasing the frequency. Dielectric constant and loss tangent of all glass added ceramics have been observed at lower frequencies (for different temperature range) and also in microwave frequency range 8.5-12 GHz (at room temperature). Highest dielectric constant and minimum dielectric loss value in microwave frequency range has been observed for BST-10P sample. Dielectric constant and loss tangent of glass added BST samples lie in the range 13.8 – 27.0 and 0.121 -0.569 respectively. Therefore, low loss ceramic material with dielectric constant in the range of 13.8 - 27.0 can be potentially useful for the design of microwave dielectric resonator antennas. Among all composition, BST-3P ceramic has been used for design and development of F-RDRA (detailed description present in chapter 5).